Journal of Electroanalytical Chemistry 709 (2013) 70–76

Contents lists available at ScienceDirect

Journal of Electroanalytical Chemistry

journal homepage: www.elsevier.com/locate/jelechem

Characterisation of screen-printed gold and gold nanoparticle-modified carbon sensors by electrochemical impedance spectroscopy

Elena Bernalte [a,*], Carmen Marín-Sánchez [a], Eduardo Pinilla-Gil [a], Christopher M.A. Brett [b]

[a] Departamento de Química Analítica, Universidad de Extremadura, Avda. de Elvas, s/n, E-06006 Badajoz, Spain
[b] Departamento de Química, Faculdade de Ciências e Tecnologia, Universidade de Coimbra, 3004-535 Coimbra, Portugal

ARTICLE INFO

Article history:
Received 11 June 2013
Received in revised form 13 September 2013
Accepted 14 September 2013
Available online 11 October 2013

Keywords:
Gold-based screen-printed electrodes
EIS
Hg

ABSTRACT

Gold-based screen-printed electrodes have been characterised by electrochemical impedance spectroscopy (EIS) to better understand their behaviour in electroanalytical applications, particularly in the anodic stripping voltammetry of Hg(II). After a first exploration by cyclic voltammetry, impedance spectra of gold-based screen-printed sensors were recorded in 0.1 M HCl electrolyte solution, in the presence of dissolved oxygen and with no electrochemical pre-treatment of the surface. The spectra demonstrated the differences in the interfacial characteristics of each kind of sensor. Structural changes in the surface of SPGEs caused by amalgam formation in the presence of Hg(II) were investigated by EIS. The results obtained were used to elucidate the implications for using the sensor in the stripping voltammetric determination of Hg(II) in environmental samples.

1. Introduction

The increasing availability of low-price homemade and commercial screen-printed electrochemical platforms has opened up new and exciting opportunities to apply electrochemical techniques outside a centralised laboratory [1–3], reinforcing one of the most important trends in analytical chemistry, and especially environmental monitoring, towards miniaturized, portable devices for on-site or even *in situ* application [4]. In this context, the great utility and versatility presented by screen-printed electrodes (SPEs) lies in the wide range of ways in which the disposable strips may be employed, as reviewed by Domínguez-Renedo et al. [5].

Despite the wide practical application of SPEs, little is known about the nature of electrode reactions at their complex surface [6]. Differences in the composition of commercial printing inks, diverse pre-treatment procedures and variable temperature conditions during the curing of the printing layer can affect their electrochemical behaviour; several studies have been performed with the aim of their characterisation [4,6–8]. In these papers, cyclic voltammetry (CV), pulse techniques such as square wave voltammetry (SWV) and scanning electron microscopy (SEM) were used for this purpose. Changes in the sensing interfacial region of the electrodes may not be observed by CV or SWV. However, they are observable by electrochemical impedance spectroscopy (EIS), owing to the wide range of timescales that this technique probes [9]. EIS has been demonstrated as a powerful tool for electrochemical characterisation [10–14].

In previous work, we have successfully demonstrated the applicability of screen printed gold electrodes (SPGE) and gold nanoparticle modified screen-printed carbon electrodes (GNP) for Hg(II) monitoring in different environmental samples [2,15–17]. As widely described, gold is the best electrode material for the electroanalytical determination of mercury, but it presents an important drawback that is the well-known phenomenon of structural changes of the surface, caused by amalgam formation with mercury [15].

Therefore, the aim of the present work was to characterise, by cyclic voltammetry and electrochemical impedance spectroscopy, three types of commercial screen-printed electrodes: high and low temperature cured screen-printed gold electrodes (SPGE-AT, SPGE-BT) and gold nanoparticles-modified screen-printed carbon electrodes (GNP). Also, the surface of SPGE-AT were also characterised by EIS in presence of Hg(II) to evaluate the influence of amalgam formation. Finally, the observation and characterisation of the gold working electrodes surfaces were also carried out by scanning electron microscopy (SEM) and X-ray photoelectron spectroscopy (XPS).

2. Experimental

2.1. Reagents and solutions

All stock and standard solutions were made from analytical grade reagents. A 10 mg/L stock solution of Hg(II) was supplied by PerkinElmer (Spain) and working solutions were prepared before measurements by dilution with ultrapure water (resistivity >18.2 MΩ cm at 25 °C) obtained from an Ultramatic system (Was-

* Corresponding author. Tel.: +34 924 289392; fax: +34 924 274244.
E-mail address: ebernalte@unex.es (E. Bernalte).

1572-6657/$ - see front matter © 2013 Elsevier B.V. All rights reserved.
http://dx.doi.org/10.1016/j.jelechem.2013.09.007

serlab, Spain). The supporting electrolyte was 0.1 M HCl (Panreac, Spain) that was demonstrated to be suitable for ASV measurements of mercury [2,15–17]. The glassware and electrochemical cell were thoroughly conditioned by cleaning with hot nitric acid (10%), rinsing with ultrapure water, drying, and keeping in hermetic plastic bags before use.

Experiments were conducted at room temperature (25 ± 1 °C) without deoxygenation.

2.2. Electrodes and electrochemical cell

Screen-printed electrodes (models 220AT, 220BT, and 110GNP) were purchased from DropSens (Oviedo, Spain). They were designed in a three electrode configuration constructed on the same ceramic platform. Working electrodes (A_{geom} = 0.126 cm^2) were composed of carbon, high and low temperature curing gold inks, and gold nanoparticles-on-carbon, respectively. Ink formulation and production characteristics of commercial SPEs are regarded by the manufacturers as proprietary information. In all of them counter and pseudo-reference printed electrodes were made of carbon (in GNP) or gold (in SPGE 220AT and 220BT), and silver, respectively. An insulating layer served to delimit the working area and silver electrical contacts of the electrode strips, connected by a special electrical connector to the potentiostat. A methacrylate voltammetric cell (DropSens, Spain) was used to perform voltammetric and EIS measurements. It is especially suitable for SPEs and designed to perform batch analysis with volumes of solution between 5 and 10 mL, with optional stirring by means of a magnetic stirrer. The screen-printed strips were immersed in the solution through a slit in the top lid leaving the electrical connections outside.

2.3. Instrumentation and methods

Voltammetric experiments were performed on a computerized hand-held, battery-powered PalmSens potentiostat/galvanostat (Palm Instruments BV, The Netherlands) interfaced with a laptop and controlled by the PalmSens PC software (PS Trace 2.5.2.0). For square-wave anodic stripping voltammetry (SWASV) the conditioning potential was +0.70 V for 15 s, deposition potential +0.20 V for 60 s, amplitude 40 mV, step potential 6 mV, frequency 20 Hz, equilibration time 10 s, and stirring rate 600 rpm [15].

Electrochemical impedance spectra were recorded using a CH Instruments 660D equipment controlled by the software provided by the supplier (CH Instruments, Inc., USA) or a Solartron 1250 Frequency Response Analyser coupled to a Solartron 1286 Electrochemical Interface (Solartron Analytical, UK), controlled by ZPlot software. The frequency range from 65 kHz to 0.1 Hz was scanned logarithmically with an applied sinusoidal perturbation of 10 mV rms amplitude in 12 steps per frequency decade, superimposed on the chosen applied potential. Data fitting to equivalent circuits was performed with CHI analyser program and ZView software, respectively. Four replicates were done at each value of applied potential to verify reproducibility of the responses.

SEM images of the working electrode surfaces were obtained by using a Hitachi FE-SEM S-4800II field emission scanning electron microscope (Tokyo, Japan). A K-Alpha X-ray photoelectron spectrometer (XPS) system (Thermo Scientific, USA) was used for X-ray surface analysis of the SPEs.

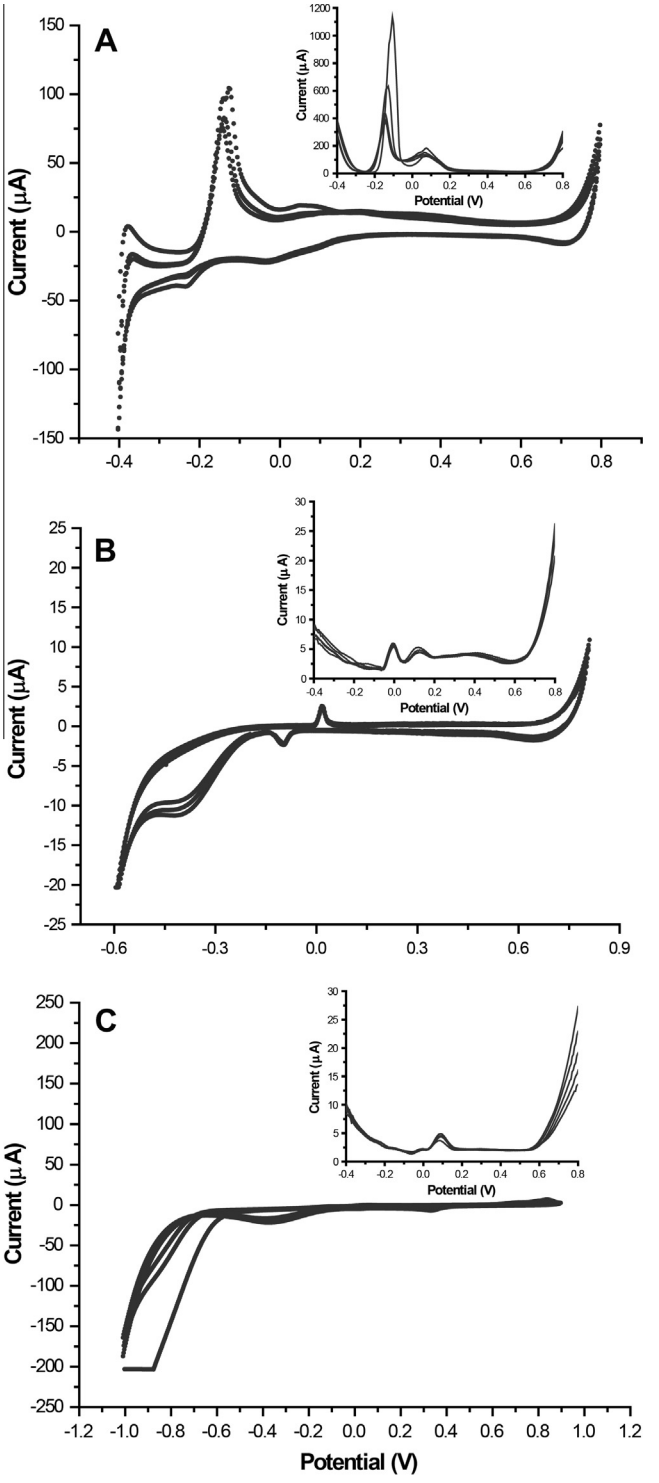

Fig. 1. Cyclic voltammograms in 0.1 M HCl at (A) SPGE-AT, (B) SPGE-BT, and (C) GNP. Scan rate 100 mVs^{-1}. Inset: square-wave anodic stripping voltammograms of 0.1 M HCl solutions. SWASV conditions: frequency 20 Hz, step potential 6 mV, amplitude 40 mV, and deposition time 60 s. Initial and final potentials were −0.4 V and 0.7 V, respectively.

3. Results and discussion

The electrochemical characterisation of the high and low temperature cured screen-printed gold electrodes (SPGE-AT, SPGE-BT) and gold nanoparticle-modified screen-printed carbon electrodes (GNP) were done by cyclic voltammetry and electrochemical impedance spectroscopy. Observation and characterisation of the working electrode surfaces were carried out by SEM and XPS, which provided morphological and microstructural information. The principal results will be discussed below.

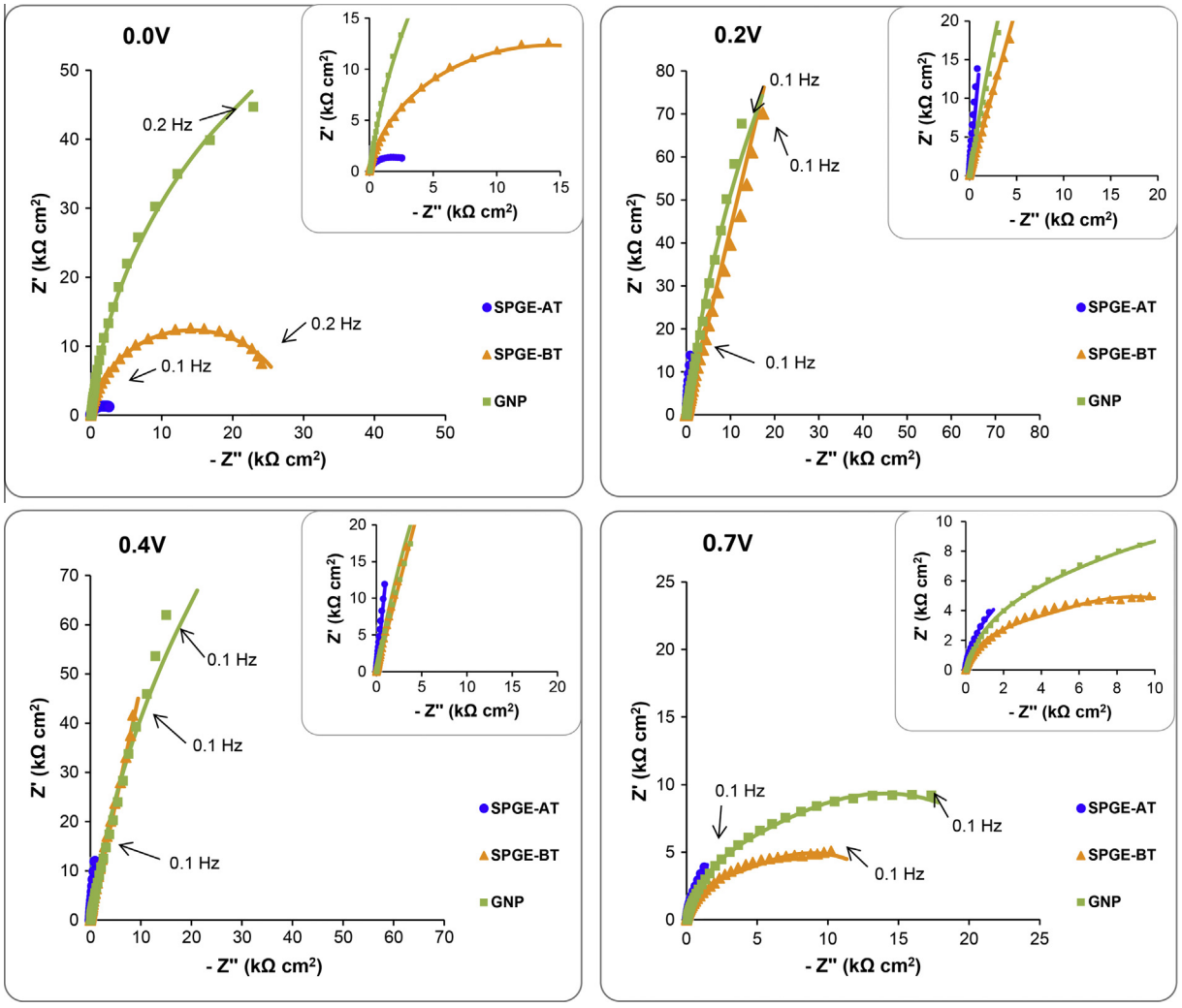

Fig. 2. Complex plane impedance spectra at 0.0, 0.2, 0.4, and 0.7 V (*vs.* pseudo Ag/AgCl) for SPGE-AT, SPGE-BT, and GNP in 0.1 M HCl. Inset plots: magnification of "high" frequency part of complex plane plots. Lines represent fitting to the equivalent circuits described in Fig. 3 and Tables 1 and 2.

3.1. Electrochemical characterisation of the SPEs

3.1.1. Cyclic voltammetry

The behaviour of bare screen-printed electrodes was first investigated by cyclic voltammetry (CV) in order to examine their potential window and the magnitude of the background currents. The information obtained was also used to establish the applied potentials to be used in the subsequent impedance experiments.

Cyclic voltammograms were recorded in 0.1 M HCl solution without pre-treatment of the working electrode surface. As expected, differences in the potential windows between different types of SPEs were significant (Fig. 1). The width of the potential windows decreased in the following order: GNP (1.9 V)>SPGE-BT (1.4 V)>SPGE-AT (1.2 V). In all SPEs, the positive potential limit remains stable around +0.8 V but the negative potential limit shifts to more positive values as the proportion of exposed gold increases. Additionally, the background current was significantly higher for SPGE-AT. The percentage of carbon present in the composition of the surface of working electrodes, as revealed by XPS: (GNP (69.9%C)>SPGE-BT (68.0%C)>SPGE-AT (27.5%C), shows that the changes in the negative potential limit can be attributed to the amount of gold and carbon exposed as well as the dispersion over the electrode surface.

Cyclic voltammograms of GNP (Fig. 1C) presents the typical behaviour of carbon electrodes. However, cyclic voltammograms of SPGE-BT (Fig. 1B) and SPGE-AT (Fig. 1A) shows an unusual peak in the positive sweep around 0.0 V, probably due to an interferent species that could be part of the gold ink formulation. Thus, square wave anodic stripping voltammograms of 0.1 M HCl solutions were recorded and the results are also shown in Fig. 1. As can be observed, the same peak at 0.1 V appeared for the three types of SPE. On the other hand, another peak appeared at 0.0 V in the stripping voltammogram of GNP, and also of SPGE-BT but with lower intensity, probably due to an oxidative process of the carbon-based film. However, the highest signal measured was observed at −0.1 V in the stripping voltammograms of SPGE-AT, that could probably be attributed to the presence of an unknown substance involved in the manufacturing of SPGE. This is in agreement with an observation reported previously [15] in which it was demonstrated that SPGE-AT could only be used at positive potentials, because irreversible changes occurred on the surface of the working electrode at negative potentials.

Based on these considerations and taking into account that the application of the SPEs is focused on Hg(II) determination by SWASV, the potentials selected for recording impedance spectra were 0.0 V (initial potential without interference signals), 0.2 V

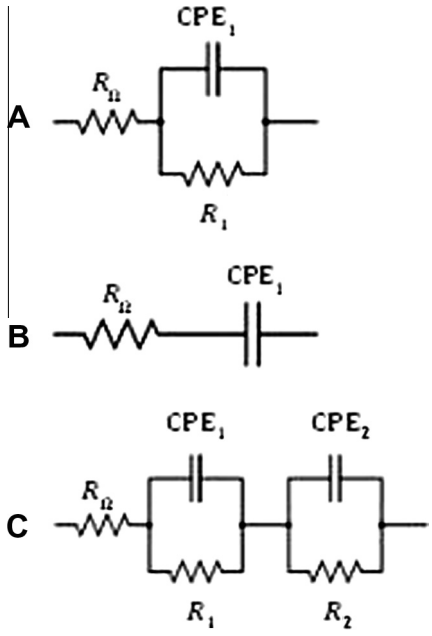

Fig. 3. Equivalent circuits for fitting impedance spectra at different applied potentials.

(potential for deposition of Hg in SWASV) [2], 0.4 (stripping peak potential of Hg by SWASV) [2,15–17] and 0.7 V (final potential).

3.1.2. Electrochemical impedance spectroscopy

Experimental complex plane impedance spectra for the bare SPGE-AT, SPGE-BT, and GNP are shown in Fig. 2 together with fitting to equivalent circuits. As seen in Fig. 2, the shape of the impedance spectra depends on the applied potential. The almost linear and close-to-vertical spectra at 0.2 V and 0.4 V indicate a purely capacitive response (with effects of surface non-uniformity) in contrast to the semicircular complex plane plots obtained at 0.0 V and 0.7 V, where both resistive and capacitive elements are important. The differences between the types of SPE are more clearly observed in the complex plane plots obtained at 0.0 V and 0.7 V.

Fitting of spectra was done using one of the three equivalent electrical circuits shown in Fig. 3, the first two of these being simplifications of the third circuit. R_Ω represents the cell resistance, R_1 and R_2 are resistances, and CPE_1 and CPE_2 are constant phase elements modelling non-ideal capacitors of capacity C_1 or C_2. The CPE exponent α represents the roughness and non-uniformity of the electrode surface, an α value of 1 corresponding to a perfectly smooth surface and of 0.5 to a porous electrode [11]. The CPEs were necessary due to the depressed semi-circle character of the responses. The results obtained are shown in Table 1. Good fits were obtained and low relative errors were found for all parameters, always less than 5%. Placing the two *R*CPE in parallel did not give good fitting to the experimental data. Thus, this circuit model can be attributed to the ink used – see further below. In general terms, the couple R_1CPE_1 would represent the surface layers of the film, and R_2CPE_2 charge transfer processes and double layer at the electrode-solution interface. Thus, at intermediate potentials where there are no charge transfer processes, the circuits in Fig. 3a or b can be employed, whereas at 0.7 V where surface oxidation can occur, it is necessary to employ the full circuit of Fig. 3c, and at 0.0 V (reduction process) for SPGE-AT.

Similar values of the cell resistance, R_Ω, of around 3 $\Omega\,cm^2$ were observed for SPGE-AT and SPGE-BT at all applied potentials tested, in contrast to the higher values of nearly 60 $\Omega\,cm^2$ obtained for GNP, that must be mainly due to the resistance of the carbon ink (SPCE gives 30 $\Omega\,cm^2$) and areas of the electrode surface which become less conducting after gold nanoparticle deposition. As seen in Table 1, immobilisation of gold nanoparticles on the surface of screen-printed carbon electrodes, gives a value of R_1 higher by a factor of a hundred, and a lower capacitance (CPE_1). The increase in R_1 can indicate a partially blocked surface with adsorbed gold nanoparticles.

A priori, the necessity of fitting using the full circuit of Fig. 3c is unexpected for SPGE-AT solid gold screen-printed electrodes for which high temperature curing of the ink is used (it is not needed for SPGE-BT, which has low-temperature curing). In agreement with the results obtained from cyclic voltammetry and anodic stripping voltammetry, this behaviour of SPGE-AT could be due to the presence of some interference involved in the printing ink manufacturing process (proprietary information).

The values of α for SPGE-AT, SPGE-BT and GNP were all around 0.9, suggesting a low degree of non-uniformity. The tendency for slightly lower values of α ($\sim$0.87) for SPGE-BT may be due to the influence of the low temperature gold curing process on the structural characteristics of the electrode. Fig. 4 presents SEM images obtained for SPGE-AT and SPGE-BT, to illustrate the differences in the surface morphology and structure of the gold working electrodes after the ink curing process. The microscopic images of SPGE-BT show a significantly greater roughness that can explain the different values of the α exponent.

3.2. Impedance in the presence of Hg(II)

As widely described in the literature, the principal drawback of the electrochemical determination of Hg(II) using solid gold electrodes is the well-known structural change of the surface due to

Table 1
Data obtained from analysis of the impedance spectra for SPGE-AT, SPGE-BT, and GNP in 0.1 M HCl and in the absence of oxygen.

Electrode	*E* (V) (*vs.* Pseudo Ag/AgCl)	R_Ω ($\Omega\,cm^2$)	CPE_1 ($\mu S\,cm^{-2}\,s^\alpha$)	α_1	R_1 ($k\Omega\,cm^2$)	CPE_2 ($\mu S\,cm^{-2}\,s^\alpha$)	α_2	R_2 ($k\Omega\,cm^2$)	Error (%)
SPGE-AT	0.0	2.8	1033	0.84	4.1	211	0.89	1.93	2.1
	0.2	2.9	118	0.95					5.1
	0.4	2.9	136	0.95					5.5
	0.7	2.7	343	0.96	16.4	4133	0.71	0.002	1.4
SPGE-BT	0.0	3.0	12.6	0.91	22.3				2.1
	0.2	2.9	18.4	0.86					3.1
	0.4	3.3	32.9	0.87					5.8
	0.7	3.0	30.3	0.87	4.0	91.0	0.87	10.73	3.6
GNP	0.0	56	23.7	0.90	140				2.9
	0.2	57	19.8	0.93	678				3.9
	0.4	57	19.6	0.92	440				4.3
	0.7	56	43.5	0.92	26.4	34.8	0.95	5.44	2.6

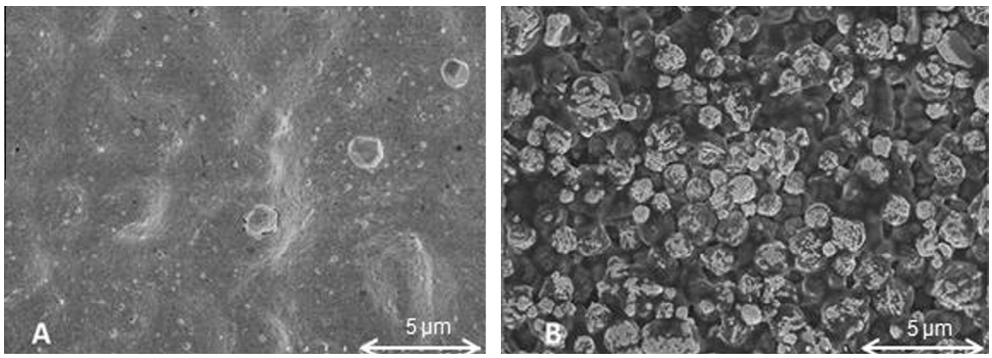

Fig. 4. SEM images obtained for (A) SPGE-AT and (B) SPGE-BT.

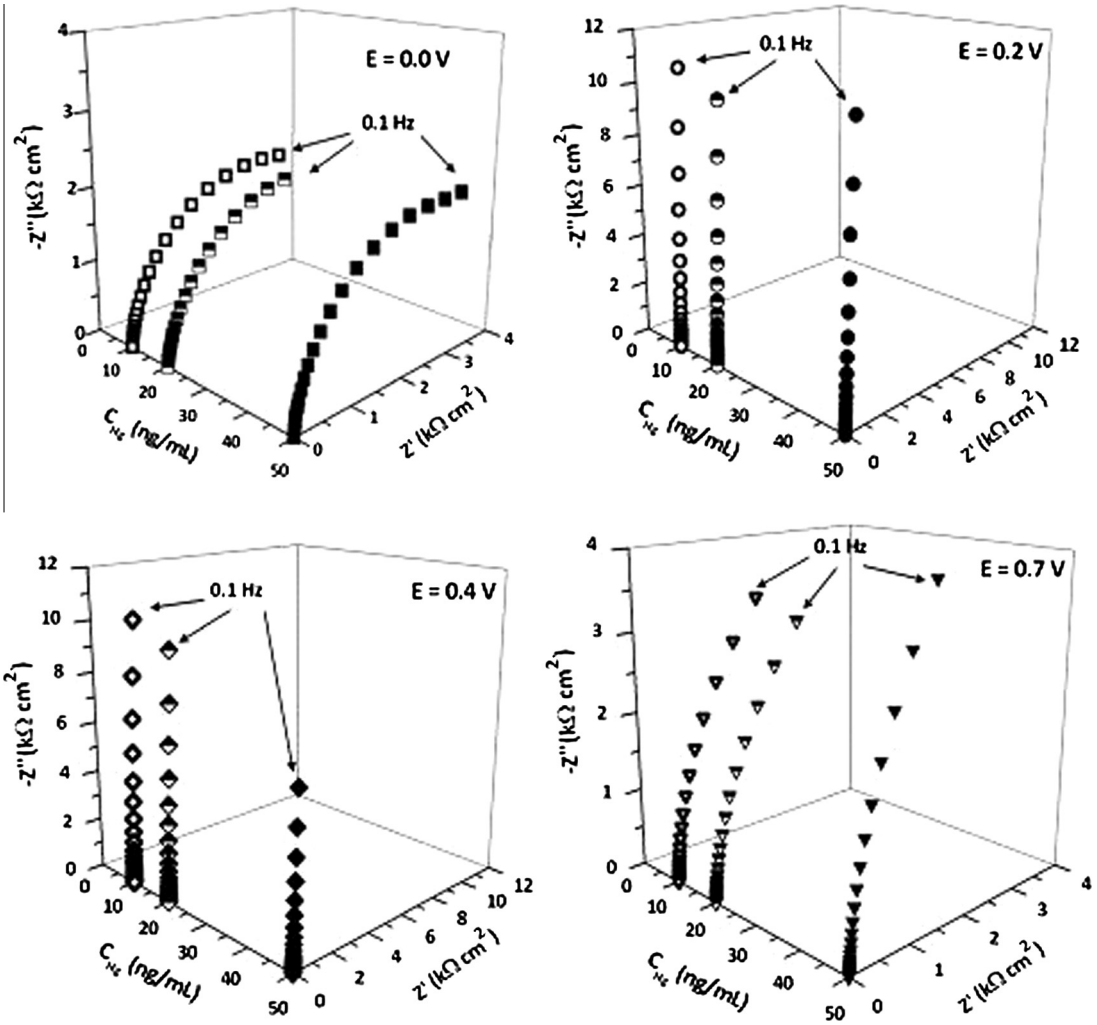

Fig. 5. Complex plane impedance plots at 0.0, 0.2, 0.4, and 0.7 V (*vs.* pseudo Ag/AgCl) for SPGE-AT in 0.1 M HCl after SW measurements in the presence of 10, 20, and 50 ng/mL Hg(II).

amalgam formation with mercury. Consequently, after the stripping voltammetric determination, the memory effect caused by amalgamation demands extensive electrochemical cleaning to recover low background currents in subsequent measurements. Therefore, electrochemical impedance spectroscopy was used to examine the reversible and/or irreversible alterations in SPGE-AT behaviour after performing SWASV in the presence of Hg(II).

The experiments were performed as follows: 10 repeated SWASV measurements, without any cleaning step between measurements, in the presence of 10, 20, or 50 ng/mL of Hg(II) were carried out successively. After that, impedance spectra (4 replicates) were recorded at 0.0 V, 0.2 V, 0.4 V, and 0.7 V, in 0.1 M HCl.

After SWASV experiments with mercury, there are changes to the surface as can be inferred, not only from visual examination of the complex plane spectra but also from the change in the equivalent circuit needed for fitting and the values of the parameters obtained. Spectra obtained for SPGE-AT are shown in Fig. 5 and the analysis of the results is given in Table 2, fitting done with an

Table 2
Data obtained from analysis of the impedance spectra for SPGE-AT in 0.1 M HCl after SWASV measurements in the presence of 10, 20, and 50 ng/mL of Hg(II).

(Hg(II)) (ng/mL)	E (V) (*vs.* pseudo Ag/AgCl)	R_Ω (Ω cm^2)	CPE$_1$ (μS cm^{-2} s$^\alpha$)	α_1	R_1 (kΩ cm^2)	Error (%)
10	0.0	2.6	168	0.93	4.4	4–8
	0.2	2.6	145	0.98		
	0.4	2.6	152	0.98		
	0.7	2.5	370	0.97	10.6	
20	0.0	2.5	233	0.92	4.3	4–8
	0.2	2.5	157	0.98		
	0.4	2.5	164	0.98		
	0.7	2.5	385	0.97	9.1	
50	0.0	2.6	170	0.94	4.4	4–8
	0.2	2.6	148	0.98		
	0.4	2.6	156	0.98		
	0.7	2.6	337	0.97	13.8	

equivalent circuit consisting of a cell resistance in series with only one parallel *R*CPE rather than two (0.0 and 0.7 V) or CPE (0.2 and 0.4 V), Fig. 3a and b. No significant overall changes in the magnitude of the impedances were observed after SWASV of Hg(II) (compare data in Tables 1 and 2), and therefore that the amalgamation of Hg with the gold working electrode does not cause any big structural changes in the surface layers of SPGE. However, some alterations must occur in the presence of metal ion, since the best equivalent circuit for modelling has just one *R*CPE, in contrast to the 2 *R*CPEs needed without mercury at 0.0 and 0.7 V. It is also seen that an increase of charge transfer resistance and a decrease of CPE occur after analysing 50 ng/mL of Hg(II), whereas lower concentrations of Hg(II) did not affect these parameters. Despite the fact that no irreversible changes take place at the surface of SPGE in the presence of low concentrations of Hg, it is seen that a relatively high concentration of the analyte (50 ng/mL) can modify the surface of the electrode, since access to the electrode is partially blocked by the amalgamation of Hg with gold, as shown in Table 2. These observations also suggest that excessive metal deposition may lead to removal of the gold surface layers and thence loss of accuracy and reproducibility of the responses.

4. Conclusions

Screen-printed electrodes based on gold cured at high (SPGE-AT) and low (SPGE-BT) temperature and carbon-modified with gold nanoparticles (GNP), were characterised by EIS. Cyclic voltammetry was used to establish the optimal potential values for performing EIS experiments.

EIS data show evidence of the differences in the behaviour of the screen-printed sensors at the different potentials monitored. GNP shows an increase in the magnitude of the charge transfer resistance and a decrease of capacitance indicating a partially blocked surface with gold nanoparticles which hinder the electron transfer. In agreement with the observations from CV, EIS results obtained for SPGE-AT can be related to the printing ink manufacturing process.

No significant changes to the surface of SPGE-AT caused by Hg(II) deposition by SWASV were demonstrated by EIS. However, the disorder caused in the surface of the electrode by deposition of a relatively high concentration of Hg(II) is manifested in the impedance spectra.

This approach based on the application of impedance spectroscopy is very useful for studying the behaviour and the properties of the gold-based screen-printed electrodes employed for *in situ* monitoring of mercury in the environment.

Acknowledgements

This work is supported by the Spanish Ministry of Science and Innovation (Project CTQ2011-25388). The authors thank the technical and human support provided by Facility of Analysis and Characterisation of Solids and Surfaces of SAIUEx (financed by UEx, Gobierno de Extremadura, MICINN, FEDER and FSE) for their assistance with SEM and XPS. E. Bernalte acknowledges a grant from Gobierno de Extremadura, Spain (PRE09107). Financial support from Fundação para a Ciência e Tecnologia (FCT), Portugal, Project PTDC/QUI-QUI/116091/2009, and PEst-C/EME/UI0285/2013, POPH (co-financed by the European Community Funds FSE and FEDER/COMPETE–Programa Operacional Factores de Competitividade), is gratefully acknowledged.

References

[1] J.P. Metters, R.O. Kadara, C.E. Banks, New directions in screen printed electroanalytical sensors: an overview of recent developments, Analyst 136 (2011) 1067.
[2] E. Bernalte, C. Marín Sánchez, E. Pinilla Gil, Gold nanoparticles-modified screen-printed carbon electrodes for anodic stripping voltammetric determination of mercury in ambient water samples, Sens. Actuators B – Chem. 161 (2012) 669.
[3] M. Li, Y.-T. Li, D.-W. Li, Y.-T. Long, Recent developments and applications of screen-printed electrodes in environmental assays – a review, Anal. Chim. Acta 734 (2012) 31.
[4] R. García-González, M.T. Fernández-Abedul, A. Pernía, A. Costa-García, Electrochemical characterisation of different screen-printed gold electrodes, Electrochim. Acta 53 (2008) 3242.
[5] O. Domínguez-Renedo, M.A. Alonso-Lomillo, M.J. Arcos-Martínez, Recent developments in the field of screen-printed electrodes and their related applications, Talanta 73 (2007) 202.
[6] P. Fanjul-Bolado, D. Hernández-Santos, P.J. Lamas-Ardisana, A. Martín-Pernía, A. Costa-García, Electrochemical characterisation of screen-printed and conventional carbon paste electrodes, Electrochim. Acta 53 (2008) 3635.
[7] R.O. Kadara, N. Jenkinson, C.E. Banks, Characterisation of commercially available electrochemical sensing platforms, Sens. Actuators B – Chem. 138 (2009) 556.
[8] R.O. Kadara, N. Jenkinson, C.E. Banks, Characterisation and fabrication of disposable screen printed microelectrodes, Electrochem. Commun. 11 (2009) 1377.
[9] C.M.A. Brett, Electrochemical impedance spectroscopy for characterisation of electrochemical sensors and biosensors, ECS Trans. 13 (13) (2008) 67.
[10] C. Gouveia-Caridade, C.M.A. Brett, Electrochemical impedance characterisation of nafion-coated carbon film resistor electrodes for electroanalysis, Electroanalysis 17 (2005) 549.
[11] C. Gouveia-Caridade, C.M.A. Brett, The influence of Triton-X-100 surfactant on the electroanalysis of lead and cadmium at carbon film electrodes – an electrochemical impedance study, J. Electroanal. Chem. 592 (2006) 113.
[12] A.P.P. Ferreira, C.S. Fugivara, S. Barrozo, P.H. Suegama, H. Yamanaka, A.V. Benedetti, Electrochemical and spectroscopic characterisation of screen-printed gold-based electrodes modified with self-assembled monolayers and Tc85 protein, J. Electroanal. Chem. 634 (2009) 111.
[13] A. Bonanni, M. Pumera, Y. Miyahara, Influence of gold nanoparticles size (2–50 nm) upon its electrochemical behaviour: an electrochemical impedance spectroscopic and voltammetric study, Phys. Chem. Chem. Phys. 13 (2011) 4980.
[14] A. Mandil, R. Pauliukaite, A. Amine, C.M.A. Brett, Electrochemical characterisation of and stripping voltammetry at screen-printed electrodes modified with different brands of multiwall carbon nanotubes and bismuth films, Anal. Lett. 45 (2012) 395.
[15] E. Bernalte, C. Marín Sánchez, E. Pinilla Gil, Determination of mercury in ambient water samples by anodic stripping voltammetry on screen-printed gold electrodes, Anal. Chim. Acta 689 (2011) 60.

[16] E. Bernalte, C. Marín Sánchez, E. Pinilla Gil, Determination of mercury in indoor dust samples by ultrasonic probe microextraction and stripping voltammetry on gold nanoparticles-modified screen-printed electrodes, Talanta 97 (2012) 187.

[17] E. Bernalte, C. Marín Sánchez, E. Pinilla Gil, High-throughput mercury monitoring in indoor dust microsamples by bath ultrasonic extraction and anodic stripping voltammetry on gold nanoparticles-modified screen-printed electrodes, Electroanalysis 25 (2013) 289.